1521-009X/42/7/1153–1162$25.00
Drug Metabolism and Disposition

http://dx.doi.org/10.1124/dmd.114.057430
Drug Metab Dispos 42:1153–1162, July 2014

Identification of a Functional Homolog of the Mammalian CYP3A4 in Locusts

Line Rørbæk Olsen, Charlotte Gabel-Jensen, Peter Aadal Nielsen, Steen Honoré Hansen, and Lassina Badolo

Department of Pharmacy, Faculty of Health and Medical Sciences, University of Copenhagen, Copenhagen, Denmark (L.R.O., C.G.-J., S.H.H.); Department of Discovery ADME, H. Lundbeck A/S, Valby, Denmark (L.B.); and EntomoPharm R&D, Lund, Sweden (P.A.N.)

Received January 31, 2014; accepted April 28, 2014

ABSTRACT

Insects have been proposed as a new tool in early drug development. It was recently demonstrated that locusts have an efflux transporter localized in the blood-brain barrier (BBB) that is functionally similar to the mammalian P-glycoprotein efflux transporter. Two insect BBB models have been put forward, an ex vivo model and an in vivo model. To use the in vivo model it is necessary to fully characterize the locust as an entire organism with regards to metabolic pathways and excretion rate. In the present study, we have characterized the locust metabolism of terfenadine, a compound that in humans is specific to the cytochrome P450 enzyme 3A4. Using high-resolution mass spectrometry coupled to ultra-high-performance liquid chromatography, we have detected metabolites identical to human metabolites of terfenadine. The formation of human metabolites in locusts was inhibited by ketoconazole, a mammalian CYP3A4 inhibitor, suggesting that the enzyme responsible for the human metabolite formation in locusts is functionally similar to human CYP3A4. Besides the human metabolites of terfenadine, additional metabolites were formed in locusts. These were tentatively identified as phosphate and glucose conjugates. In conclusion, not only may locusts be a model useful for determining BBB permeation, but possibly insects could be used in metabolism investigation. However, extensive characterization of the insect model is necessary to determine its applicability.

Introduction

Today, most new drugs that fail in the clinical phase do so due to lack of desired pharmacological activity or toxicity (Hughes et al., 2011). In the development of central nervous system drugs, the blood-brain barrier (BBB) creates additional challenges, and therapeutic agents for the treatment of neurologic disorders often fail in clinical trials due to inadequate BBB permeation (Alavijeh et al., 2005; Geldenhuys et al., 2012). In vitro methods for testing BBB penetration are too simple, not integrating the complexity of the BBB, and therefore may lack important functions of the BBB (Naik and Cucullo, 2012). Preclinical in vivo models are very costly in terms of time and use of animals (rodents). Fast screening models for BBB permeation are therefore very attractive.

Insects have been suggested as novel models in drug discovery (Geldenhuys et al., 2012). It has been demonstrated that locusts, among other insects, have an efflux transporter that is functionally similar to the mammalian P-glycoprotein efflux transporter (Nielsen et al., 2011).

Currently, two insect BBB models have been reported using locusts as model insects (Nielsen et al., 2011; Andersson et al., 2013). An ex vivo model has been developed and allows application of test items directly to entire brains isolated prior to testing. Besides this model, an in vivo model has also been developed in which the test item is injected in the hemolymph and may need to pass the barriers of metabolism and excretion before reaching the brain. As such, the in vivo locust model may have more similarities to other in vivo models like rodent models. Also, the brain remains in its natural environment, with no risk of impairing the barrier function.

Despite obvious anatomic differences, there are many physiologic and biochemical similarities between insects and mammals. Essential systems such as protein synthesis and cell metabolism are not significantly different between insects and mammals (Klowden, 2007). Monooxygenases like the cytochrome P450 (P450) enzymes are found in virtually all eukaryotic organisms, including insects (Scott, 2008). This is of specific interest as some of the most important drug-metabolizing enzymes in humans are the P450 enzymes. Among mammalian P450 enzymes, the subfamilies CYP1A1/2, CYP2B6, CYP2C9/19, CYP2D6, CYP2E1, and CYP3A4/5 are the main contributors, and CYP3A4 accounts for the metabolism of almost half of all marketed drugs (Guengerich, 2008).

Most literature on insect metabolic systems concerns insecticide detoxification mechanisms and resistance development (Smith, 1962; Wilkinson and Brattsten, 1972; Feyereisen, 1999; Scott and Wen, 2001). Furthermore, most research was conducted in the 1950s and 1960s when the analytic methods were limited compared with the technologies available today.

In the present study, we have characterized the metabolism in locusts of the antihistaminic drug terfenadine, a specific human CYP3A4 substrate.

This work was supported by the Danish National Advanced Technology Foundation [Grant 023-2011-3].
dx.doi.org/10.1124/dmd.114.057430.

ABBREVIATIONS: AUC, area under the curve; BBB, blood-brain barrier; DMSO, dimethylsulfoxide; HLM, human liver microsome; MS, mass spectrometry; MS^2, tandem mass spectrometry; P450, cytochrome P450.

Materials and Methods

Solvents and reagents: All solvents used were at least of high-performance liquid chromatography grade. Methanol (MeOH) was purchased from BDH Prolabo (VWR, Herlev, Denmark). The following reagents were purchased from Sigma-Aldrich (St. Louis, MO): female pooled human liver microsomes (HLMs), glucose 6-phosphate, glucose-6-phosphate dehydrogenase from Baker's yeast, $NADP^+$, formic acid, $MgCl_2 \bullet 6H_2O$, quinidine, α-naphthoflavone, sulfaphenazole, nootkatone, ketoconazole, and amitriptyline. The following were purchased from Merck (Darmstadt, Germany): $K_2HPO_4 \bullet 3H_2O$, KH_2PO_4, $ZnSO_4 \bullet 7H_2O$, and dimethylsulfoxide (DMSO). Terfenadine was provided by NeuroSearch A/S (Ballerup, Denmark). Water for mobile phases and solutions was purified with the Direct-Q 3 UV system (Millipore, Billerica, MA).

Animals: Male desert locusts, *Schistocerca gregaria* (L), were obtained from a commercial breeder (Petra Aqua, Prague, Czech Republic). The locusts were housed under crowded conditions in a 12-hour light/dark cycle at 25–35°C. They had constant access to Chinese cabbage and dried wheat bran. Experiments were carried out on fed fifth instar locusts aged 3–5 weeks after final molt.

Locust experiments: Terfenadine, quinidine, sulfaphenazole, nootkatone, α-naphthoflavone, and ketoconazole were dissolved in DMSO and diluted with 0.1% lactic acid in Milli-Q water (Millipore) to the applied concentrations. Terfenadine was administered alone or in a cosolution with one of the following P450 inhibitors: ketoconazole, quinidine, sulfaphenazole, nootkatone, or α-naphthoflavone. DMSO concentrations in all solutions used for injection were 7.5% due to low solubility of some of the inhibitors. The locusts contained ~144 μl hemolymph per g (Lee, 1961) and had an average weight of 1.59 ± 0.166 g (mean ± S.D.; $n = 10$), and thus the final DMSO concentration in hemolymph was expected to be <2%.

The locusts were injected with 40 μl of 500 μM terfenadine (with and without 2.5 mM inhibitor) between two terga and kept fixated at room temperature during the experiment. The effects of different P450 inhibitors were determined using a hemolymph sample 60 minutes postinjection ($n = 4$). If significant inhibition of terfenadine metabolism was observed, time profiles of metabolites formed were obtained from hemolymph samples over a time period of 2 hours. Hemolymph samples were taken from the locust at 1, 5, 10, 20, 30, 45, 60, and 120 minutes postadministration. Samples were collected using an end-to-end micropipette (10 μl) through a small hole punctured in the soft tissue below the head. The collected hemolymph was added to 40 μl of 2% $ZnSO_4$ in 50% MeOH (on ice) containing amitriptyline as internal standard. After 120 minutes, the locusts were euthanized by freezing. For detection of metabolites in feces, locusts were dosed with 40 μl of 500 μM terfenadine (with or without 2.5 mM inhibitor) and left for 24 hours. Then feces were collected and weighed and metabolites were extracted with 50% MeOH-containing internal standard by ultrasonication for 30 minutes.

All samples collected were stored at −18°C prior to analyzing. After thawing, the hemolymph samples were centrifuged for 10 minutes at 15,000*g* at 5°C and the supernatants transferred to vials for analysis. The fecal extracts were filtered through 0.45-μm Millex-HV syringe filters (Millipore) and analyzed. Hemolymph and feces from nontreated locusts were used as controls.

HLM incubation method: HLMs (0.5 mg/ml) were preincubated at 37°C for 5 minutes in 100 mM potassium phosphate buffer (pH 7.4) with 3.3 mM $MgCl_2$, 0.4 U/ml glucose-6-phosphate dehydrogenase, 3.3 mM glucose 6-phosphate, and 1.2 mM $NADP^+$. After preincubation, terfenadine was added (final concentration, 4 μM). Samples (20 μl) were taken out at the same time points as for the locust experiments, and the reaction was quenched using 80 μl of 2% $ZnSO_4$ in 50% MeOH and containing 3% formic acid (on ice). The samples were stored at −18°C.

After thawing, the samples were centrifuged for 10 minutes at 15,000*g* at 5°C and the supernatants analyzed with liquid chromatography–mass spectrometry (MS).

To determine pharmacokinetic parameters (K_m) in locusts, five different terfenadine concentrations were used (250, 500, 1000, 1500, and 2500 μM). The concentration of DMSO was kept at 2.5% (<0.2% in hemolymph). Terfenadine solution (40 μl) was injected, and after 1 minute 20 μl of hemolymph was drawn from the locusts and added to 80 μl of 2% $ZnSO_4$ in 50% MeOH containing internal standard. The samples were prepared in a Sirocco 96-well plate for protein precipitation (Waters, Milford, MA). The plate was centrifuged at 2000*g* for 4 minutes, and the filtrate was collected and analyzed.

TABLE 1

MS settings for identification of metabolites

	Full Scan	dd-MS^2	tMS^2
Resolution	70,000	17,500	17,500
AGC target	3e6	1e5	2e5
Maximum injection time (ms)	100	50	100
Scan range	200–750	—	—
Isolation window	2.0 *m/z*		1 *m/z*
NCE	—	35	35
Underfill ratio		0.1%	

dd-MS^2, data-dependent tandem MS; tMS^2, targeted tandem MS.

Ultra-high-performance liquid chromatography–MS method: The chromatographic separation was performed on a Kinetex C_{18} (50 × 2.1 mm) column (Phenomenex, Torrance, CA) with 1.7-μm particles using a Dionex UltiMate 3000 RS ultra-high-performance liquid chromatography system (Thermo Scientific, Waltham, MA) coupled to a high-resolution MS instrument [Q Exactive Orbitrap with a HESI-II interface from ThermoFinnigan (San Jose, CA)]. Separation was performed with gradient elution using 0.1% formic acid in Milli-Q water as mobile phase A and MeOH with 0.1% formic acid as mobile phase B with a flow rate of 0.4 ml/min. The mobile phase B was kept at 5% for 0.2 minutes followed by a linear gradient of 5%–90% B over 5 minutes, 90% B for 1 minute, followed by re-equilibration for 2 minutes. The column compartment was set to 30°C, and the samples were kept at 8°C.

Detection of metabolites was performed in positive ionization mode using data-dependent tandem MS (MS^2) on the top five most abundant ions in each scan with an dynamic exclusion of 5 seconds. Quantification of terfenadine was performed in targeted MS^2. The lock mass used (214.0896 *m/z*) originated from a plasticizer, *N*-butyl benzenesulfonamide. MS settings were as shown in Table 1. Spray voltage was set to 3.3 kV, capillary temperature 350°C, sheath gas 30 arbitrary units, auxiliary gas 10 arbitrary units, probe heater 250°C, and S-lens RF level 50. Thermo Scientific Mass Frontier 7.0 Spectral Interpretation Software was used for identification of metabolites.

For statistical evaluation, a Student's *t* test was used.

Results

HLM Metabolites

To investigate whether metabolites obtained in the locust were similar to those obtained in humans, HLMs were incubated with the test compound and the metabolites obtained here were used as reference compounds in comparison with locust metabolites. The phase I metabolites most frequently reported in the literature are shown in Fig. 1 and were all detected in HLMs and confirmed by

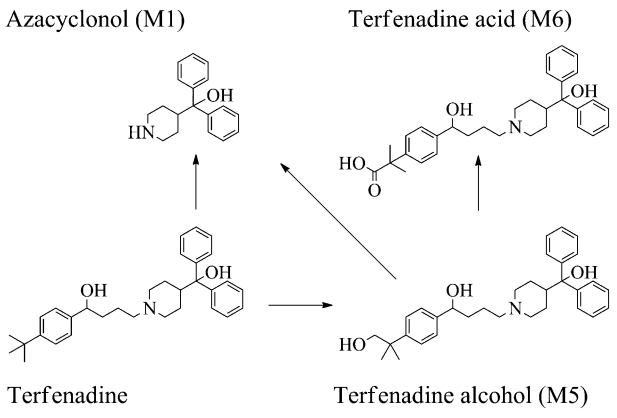

Fig. 1. Structures of terfenadine and known metabolites formed in mammals by CYP3A4 (Jurima-Romet et al., 1994; Ling et al., 1995; Rodrigues et al., 1995).

TABLE 2

Metabolites identified in locust feces and HLMs

Compound	Retention time for metabolites identified in locust hemolymph and/or feces	Retention time for metabolites identified in HLMs	Parent *m/z*	Major Fragment *m/z*	Other Fragment *m/z*
	min				
M1 (azacyclonol)	3.45	3.47	268.170	250.159	167.085
M2	3.79	3.81	504.311	468.289	486.299, 262.158, 89.060
M3	4.15	N.F.	650.369	452.294	632.357, 614.345, 470.305, 262.158, 73.065
M4	4.16	N.F.	504.310	262.159	486.230, 468.289, 89.060
M5 (terfenadine alcohol)	4.27	4.30	488.317	452.294	470.305, 262.159, 73.065
M6 (terfenadine acid)	4.30	4.33	502.295	466.274	484.284, 262.159, 87.045
M7	4.45	4.49	486.301	219.138	468.289
M8	4.47	4.51	500.280	233.117	482.270
M9	4.51	N.F.	568.283	532.261	550.271, 488.315, 470.305, 452.295, 262.159, 98.985
M10	4.74	N.F.	634.374	436.299	616.360, 454.310, 262.159, 57.071
M11	4.74	N.F.	566.267	201.127	548.256, 299.104, 98.985
Terfenadine	4.91	4.94	472.321	436.299	454.310, 262.158, 57.071
M12	5.43	N.F.	552.289	436.299	454.309, 262.158, 57.071

N.F., not found.

accurate mass and fragmentation patterns (Jurima-Romet et al., 1994; Ling et al., 1995; Rodrigues et al., 1995).

Observed fragmentation patterns of terfenadine and metabolites are given in Table 2. Other metabolites and/or intermediates (M2, M7, and M8) were also identified in HLMs. M1, M5, and M6 were identified as azacyclonol, terfenadine alcohol, and terfenadine acid, respectively, and the structures are shown in Fig. 1.

Substrate Specificity in Locusts and Mammals

To determine whether there is an enzyme in locusts with the same substrate specificity as found in mammals, terfenadine was administered by intrahemolymphic injection alone or along with each of five inhibitors known to inhibit different P450 enzymes (given in parentheses) involved in drug metabolism: α-naphthoflavone (1A2), sulfaphenazole (2C9), nootkatone (2C19), quinidine (2D6), and ketoconazole (3A4). The results are shown in Fig. 2. Only coadministration with ketoconazole resulted in a significant inhibition of formation of metabolites in locusts. The terfenadine dose given to the locusts corresponds to the weight-adjusted daily oral dose in humans (120 mg $\approx$ 2 mg/kg) but dosed directly in the hemolymph.

Elimination of terfenadine from locust hemolymph was followed over time (Fig. 3), and the area under the curve (AUC) with and without coadministration of ketoconazole was calculated. As can be seen in Fig. 3B, the AUC was significantly (1.7-fold) larger when ketoconazole was coadministered.

Detection of P450 Metabolites in Locusts

Metabolites were detected in locust hemolymph and feces with fragmentation patterns and retention times identical to metabolites identified in HLM incubations. The metabolites were not quantified; however, the relative amounts of the different metabolites were different in hemolymph and feces. Thus, M1 and M6 were the most abundant in hemolymph, whereas M5 was more abundant in feces. M2, M3, M4, and M7 were identified only in feces. M3, M4, M9, M10, M11, and M12 were detected only in locusts.

M1, M5, M6, and M8 were all found in HLM incubations and in locust hemolymph as well as locust feces. M1, M6, and M8 increased over time when no inhibitor was coadministered, as can be seen in Fig. 4. In locust hemolymph, M5 increased rapidly in the first 5 minutes and then decreased over time. This was also seen in HLM incubations, although in the latter the decrease started after 20 minutes. The formation of all four metabolites was inhibited almost completely by coadministration of ketoconazole.

Detection of Non-P450 Metabolites

Non-P450 metabolites were identified based on similarities in fragmentation patterns, as seen in Table 2. Besides the six metabolites identified in HLM incubations, an additional six metabolites were detected in locusts. Only four of these metabolites were detected in hemolymph in sufficient concentrations to be measured over time (Fig. 5).

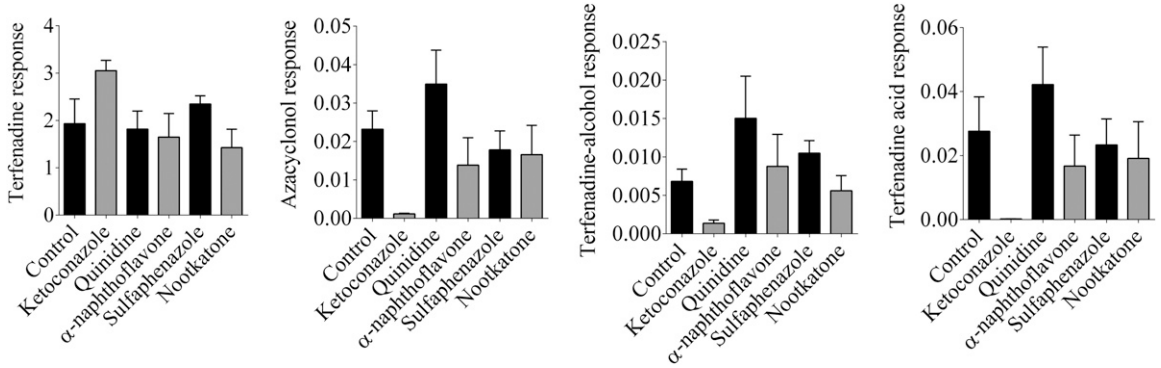

Fig. 2. Response of terfenadine and known mammalian metabolites after administration of terfenadine to locusts with and without coadministration of inhibitors. Data are means and S.E.M.; $n = 4$.

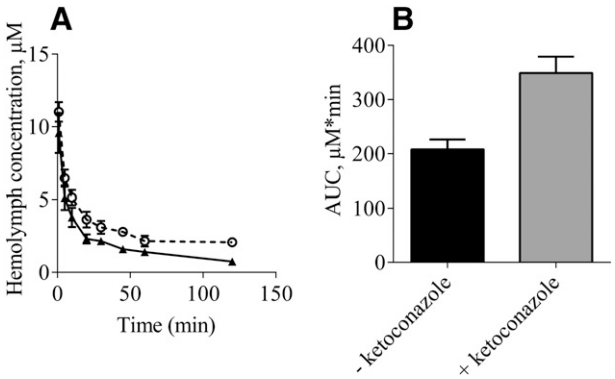

Fig. 3. Elimination of terfenadine from hemolymph (A) and calculated AUCs (B). Results with (▲) and without (○) the inhibitor ketoconazole. Data are means and S.E.M.; $n = 6$.

The excreted amount of unchanged terfenadine was not significantly different with and without coadministration of ketoconazole, ranging from 3%–30% of the administered dose (data not shown). The excretion of only one metabolite was significantly increased when ketoconazole was coadministered (M10). The formation of M12 appears to be inhibited by ketoconazole; however, the excreted amount of this metabolite was not significantly different (Figs. 5 and 6). The rest of the metabolites were inhibited (M7, M8, M9, and M11) or not affected (M3). M2 and M4 were also significantly inhibited by ketaconazole; however, the responses of these metabolites were very low compared with the rest of the metabolites and therefore are not included in the figures.

Metabolite Identification

A spectrum of M3 (*m/z* 650) is shown in Fig. 7. Fragmentation of M3 is almost identical to the fragmentation of M5, suggesting that M3 is a conjugate of M5 ($\Delta m/z = 162$). M3 was identified in locust feces, and the amount excreted was not significantly changed when ketoconazole was coadministered. In hemolymph, the concentration was too low to be followed over time, suggesting that the excretion rate for this metabolite is high or that M3 is further metabolized.

As mentioned, the different metabolites were not quantified; however, based on the MS response, M9, with an accurate mass of 568.281, was the most abundant metabolite found in locust feces and hemolymph. As seen in Fig. 8, the fragmentation pattern resembles the fragmentation for terfenadine alcohol (M5). The fragment of 73 *m/z* is missing, and an additional fragment of 99 *m/z* can be seen. In Figs. 5 and 6 it appears that the formation of M9 is significantly inhibited by ketoconazole.

M10 was identified as a direct conjugate of terfenadine without any prior phase I modification. According to Table 2, the mass of M10 corresponds to the *m/z* of terfenadine + 162 Da. The fragmentation pattern for fragments with $m/z < 472$ was identical to terfenadine. In Fig. 5 it can be seen that the formation rate of M10 was not affected by ketoconazole in the first 20 minutes postinjection. From 20 minutes the amount of M10 increased significantly compared with the amount

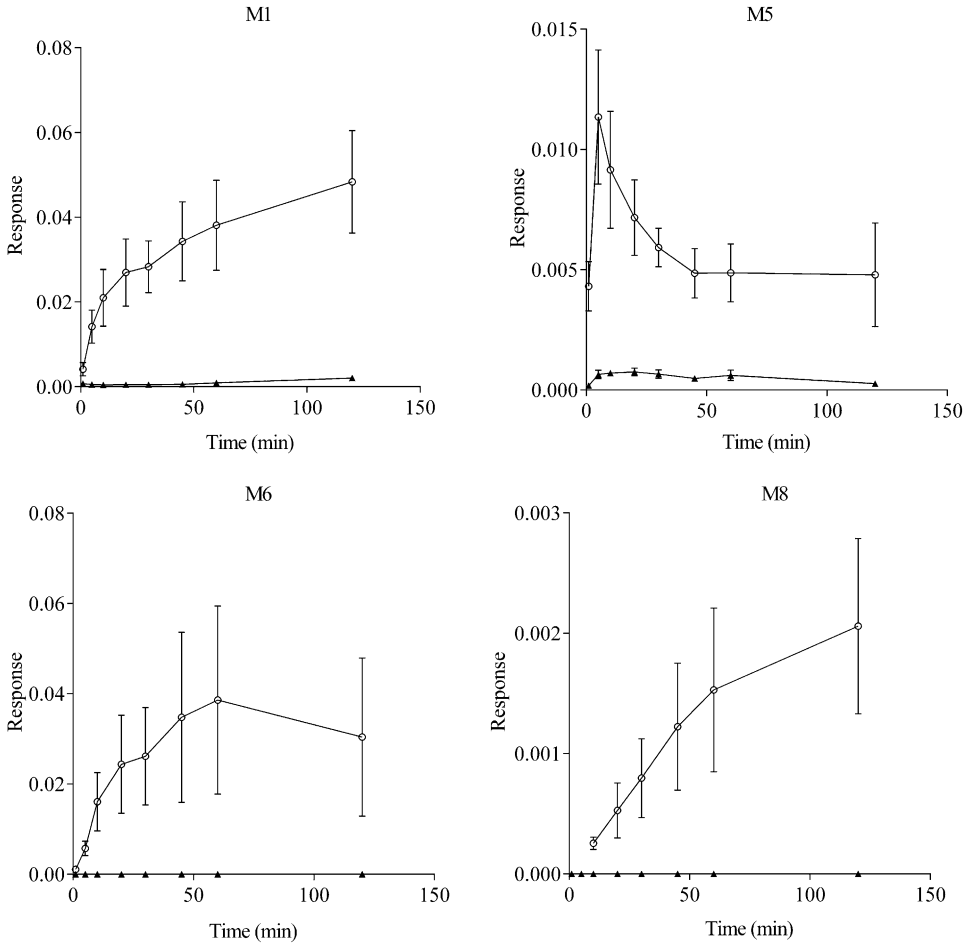

Fig. 4. Major metabolites identical to HLM metabolites identified in locust hemolymph over time. Results with (▲) and without (○) inhibitor. Data are mean and S.E.M.; $n = 6$.

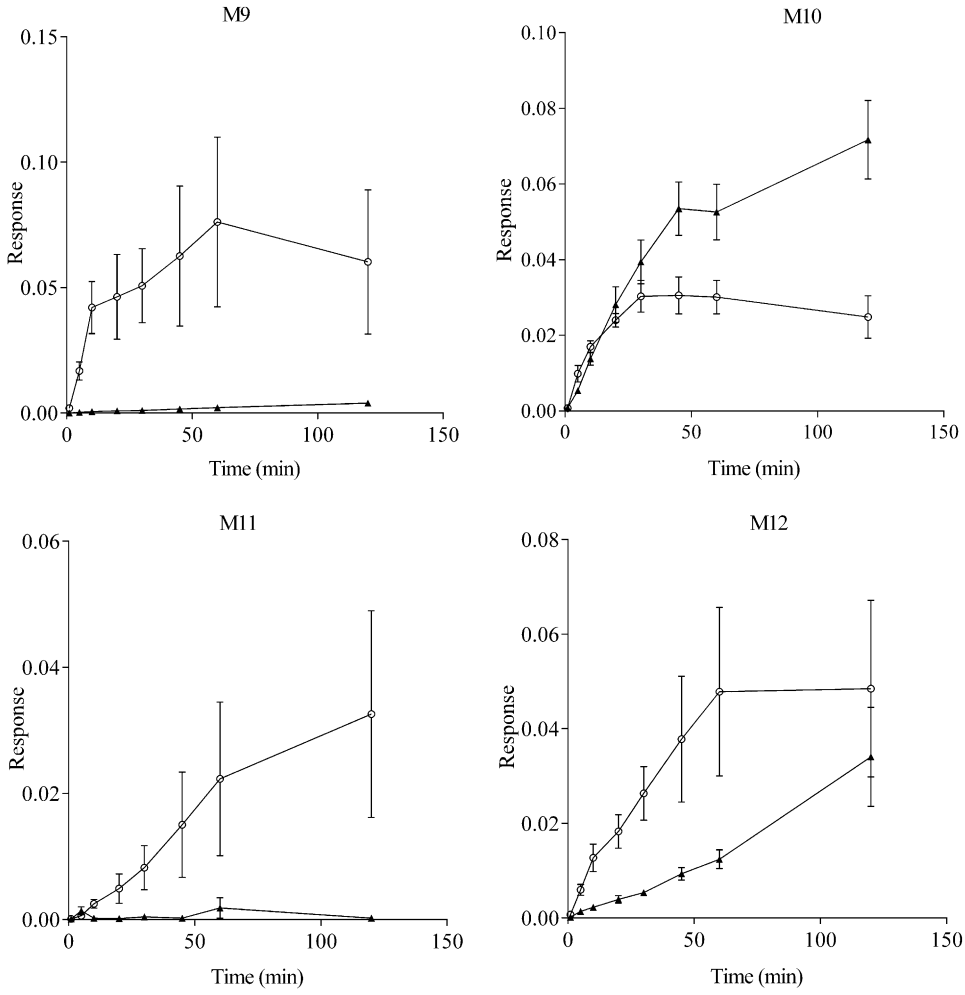

Fig. 5. Major non-P450 metabolites identified in locust hemolymph over time. Results with (▲) and without (○) inhibitor. Data are mean and S.E.M.; $n = 6$.

in locusts receiving only terfenadine. The amount of excreted M10 was increased in locusts coadministered ketoconazole.

M11 shares some of the fragments seen for M7 and is expected to be a conjugate of M7. Fragmentation patterns were not similar regarding fragments with $m/z < 450$. As can be seen in Figs. 5 and 6, formation of M11 is inhibited by ketoconazole.

M12 is expected to be a direct conjugate of terfenadine. The fragment of 472 (m/z of terfenadine) is missing in the MS^2 spectrum of M12, and only one water molecule is lost. Furthermore, a fragment of 98.99 m/z was observed. The formation of this metabolite in hemolymph was initially inhibited by ketoconazole (Fig. 5). No significant difference could be shown for the amount excreted in feces when the locusts were given ketoconazole (Fig. 6).

Metabolite ID

Phase I Metabolites. The fragmentation patterns of M1, M5, and M6 are described in the literature, and these are consistent with the observed fragmentation pattern (Rodrigues et al., 1995). The

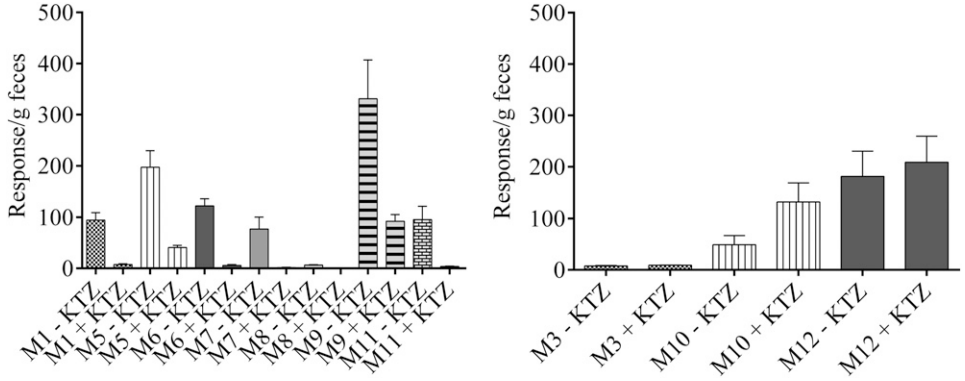

Fig. 6. MS response of terfenadine and the most abundant metabolites identified in feces collected from locusts 24 hours after injection (with and without coadministration of inhibitor). (Left) The metabolites significantly inhibited by coadministration of ketoconazole; (right) the metabolites unaffected or increased. Four locusts per cage. Data are mean and S.E.M.; $n = 3$. KTZ, ketoconazole.

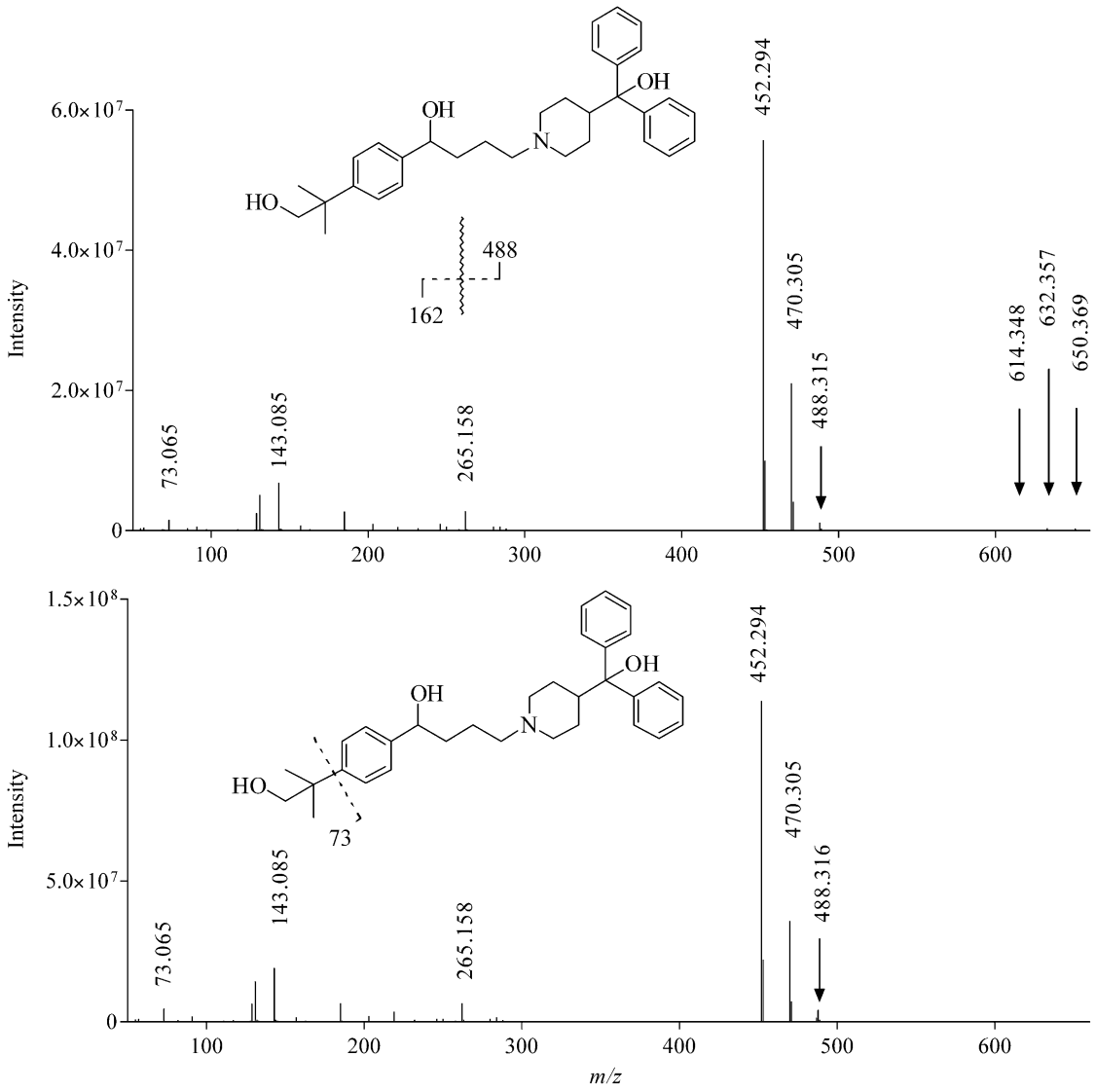

Fig. 7. Fragmentation pattern of M3 (top), with parent mass of 650.369, and M5 (bottom), with parent mass of 488.316.

fragmentation pattern of terfenadine has a characteristic loss of two consecutive water molecules from the parent mass, and the *tert*-butyl group results in a fragment with *m/z* of 57. The fragmentation patterns of M5 and M6 show that the parent masses have shifted but there is still consecutive loss of two water molecules. The primary alcohol on M5 is too stable to result in a loss of water. The *tert*-butyl fragment of *m/z* 57 has shifted according to the metabolic modification, thus confirming where oxidation has taken place. Full structural elucidation by NMR of metabolites was not attempted, and authentic standards were not available. Instead, fragmentation patterns and accurate mass were used for identification.

The MS responses of M2, M7, and M8 were minor and expected to be intermediates, as reported by Jurima-Romet et al. (1994). M2 appears to be a double-hydroxylated metabolite. Both hydroxylations occur on the *tert*-butyl group, as a fragment of 89.060 *m/z* (57 + 16 + 16) was identified. The exact mass of M7 corresponds to an aldehyde and M8 to an acid-ketone metabolite. M4 has the same accurate mass as M2 but was only detected in locust feces. As with M2, the fragmentation pattern suggests that this metabolite could be a double-hydroxylated compound; however, the fragmentation pattern was slightly different compared with M2 (Table 2).

Phase II Metabolites (Locusts Only)

Glucosylation. The metabolites M3 and M10 were only formed in locusts and were tentatively identified as glucosides of M5 and terfenadine, respectively. The mass accuracy was better than 0.1 ppm. The glucose conjugation site of M10 could be the amine or one of the secondary alcohols. Although highly speculative, it could be suggested that the glucosylation occurs on the latter as there is only a single loss of water from M10 (634 → 616). The fragmentation pattern of M10 was identical to the fragmentation pattern of terfenadine for $m/z < 472$.

Regarding M3, it can be seen in Fig. 7 that there is a consecutive loss of two water molecules (650 → 632 → 614), suggesting that the glucose is conjugated to the nitrogen or the primary alcohol. The fragment with *m/z* 73 is formed, confirming that the hydroxylation has occurred on the *tert*-butyl group of terfenadine.

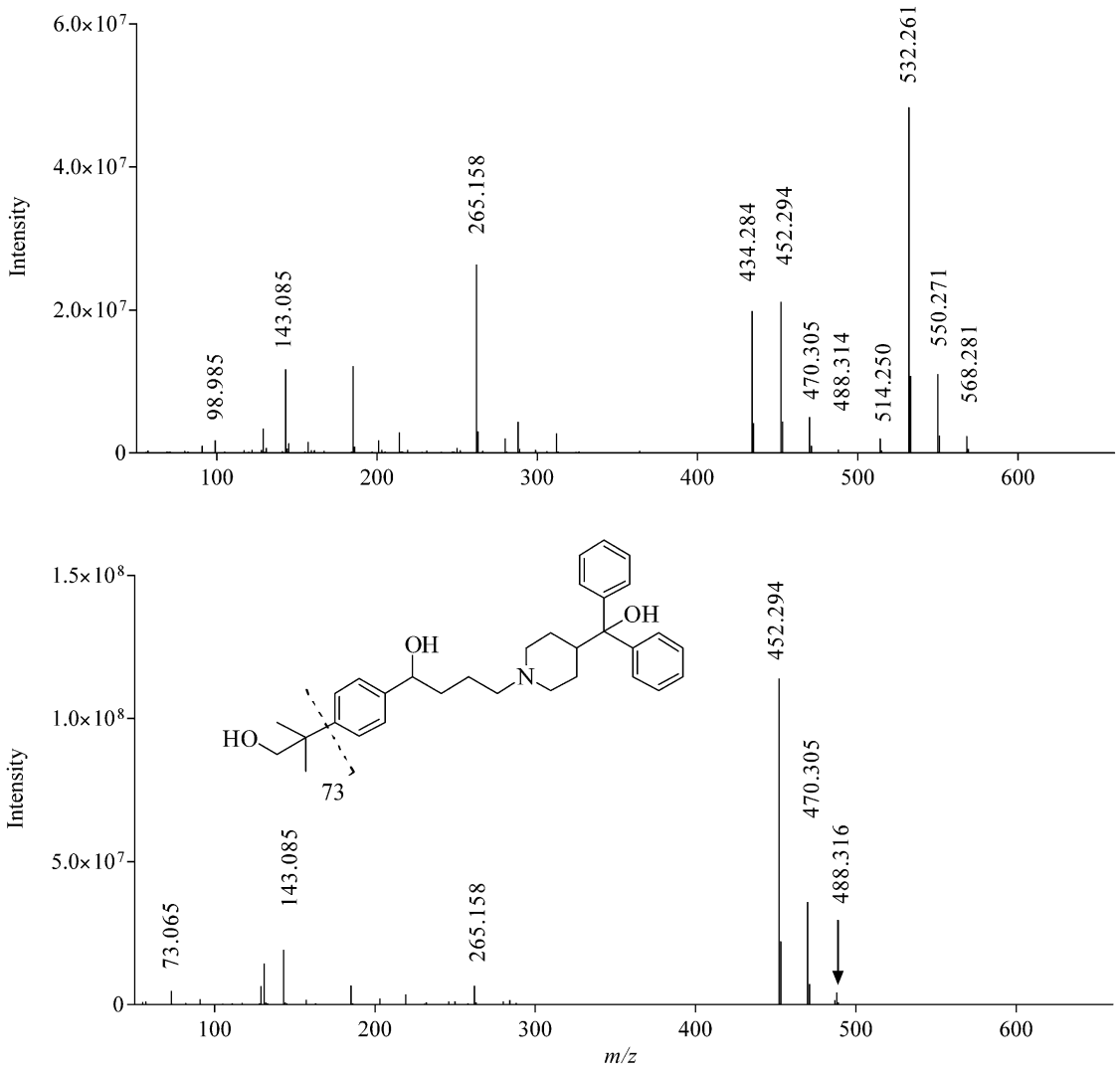

Fig. 8. MS/MS spectrum of M9, with parent mass of 568.281 (top), and M5, with parent mass 488.315 (bottom).

Phosphorylation. M9, M11, and M12 were tentatively identified as phosphate esters of terfenadine alcohol, M7, and terfenadine, respectively. The mass accuracy was better than 0.5 ppm. Two consecutive water molecules are readily lost from M9, indicating that the phosphate ester is conjugated to the primary alcohol of M5 (Fig. 8). The fragment of 434 (M5 – $3H_2O$) is not seen in the MS/MS spectrum of terfenadine alcohol (M5). The fragment is, however, seen in the spectrum of M9, suggesting that the phosphate group is more readily lost by fragmentation. Also, the fragment at *m/z* 73 indicating a hydroxylation on the *tert*-butyl group is also missing, indicating that the entire phosphate group is lost. The same pattern was observed for M12, where the fragment of 472 (*m/z* of terfenadine) is missing in the MS/MS spectrum of M12. Only one water molecule is lost, suggesting that the phosphate forms an ester with one of the existing hydroxyl groups in the molecule. In the MS/MS spectra of all the phosphorylated metabolites a fragment of 98.99 *m/z* could be seen. This fragment is thought to originate from protonated phosphate ($H_4PO_4^+$).

A proposed metabolic pathway of terfenadine in locusts can be seen in Fig. 9.

Pharmacokinetic Parameters

Due to extensive phase II metabolism of both parent and phase I metabolites, a measure of the initial formation rate had to be done within 1 minute. At this time point, substantial interindividual variation was observed. Hence, estimation of pharmacokinetic parameters was not successful.

Discussion

Human phase I metabolites of terfenadine were produced in HLMs and used as references to identify and characterize the metabolites in locusts. Metabolites identical to the metabolites detected in HLM incubations of terfenadine (M1, M2, M5, M6, M7, and M8) were identified in locust hemolymph and feces after administration of the drug. In humans, terfenadine is metabolized almost exclusively by CYP3A4 into the metabolites shown in Fig. 1. Human data have shown increases in terfenadine AUC, after multiple dosing, ranging from 16 to 73 times when CYP3A4 is inhibited by ketoconazole (Honig et al., 1993); however, unchanged terfenadine is normally undetectable in plasma due to extensive first-pass metabolism

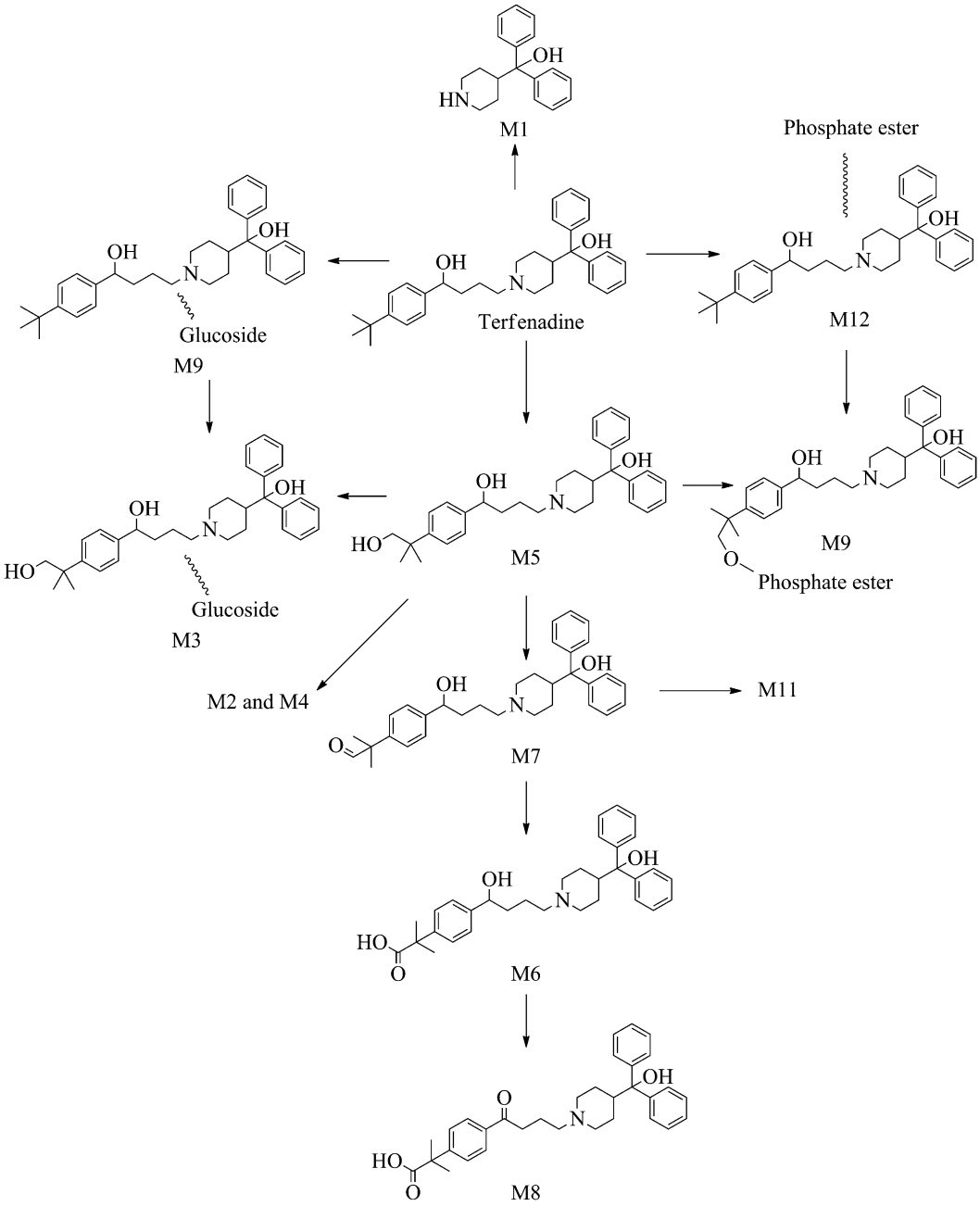

Fig. 9. Proposed metabolic pathways and structures of locust metabolites.

(Jurima-Romet et al., 1994). In in vitro assays using cryopreserved human hepatocytes, ketoconazole provides almost complete inhibition of terfenadine metabolism (Shibata et al., 2008). In HLMs, the response of azacyclonol (M1) increased over time in both HLM incubations and locust hemolymph. Terfenadine alcohol (M5) rose in the first 20 minutes and then declined, indicating that this metabolite is further converted. The same was seen in locust hemolymph, only the decline started after 5 minutes. Terfenadine acid (M6) and M8 increased after a short lag time in both HLM incubations and locust hemolymph, suggesting that M5 (terfenadine alcohol) was further converted into these metabolites. In vivo K_m values for the formation of phase I metabolites are not reported, as unchanged terfenadine usually is undetectable in plasma when given in therapeutic doses (Jurima-Romet et al., 1994). In vitro data obtained using human liver microsomes resulted in K_m values for azacyclonol between 0.82 and 11 μM. The K_m values for hydroxy-terfenadine formation in human liver microsomes ranged between 1.8 and 18 μM (Raeissi et al., 1997; Jurima-Romet et al., 1998).

Because no in vivo data are available for comparison and because the in vitro data vary considerably, no further attempt to establish kinetic parameters for the metabolite formation was performed.

When locusts were exposed to a single dose of terfenadine combined with different P450 enzyme inhibitors, it was only ketoconazole (an inhibitor of CYP3A4) that inhibited the formation of the mammalian metabolites, indicating that the formation of these metabolites in locusts is catalyzed by an enzyme functionally related to mammalian CYP3A4. As can be seen in Fig. 3B, the AUC is significantly (1.7-fold) larger when ketoconazole is coadministered, indicating that the

elimination of terfenadine is inhibited. The excreted amount of terfenadine is not changed, and compared with the inhibition observed in humans, the increase in AUC in the locusts is moderate, indicating that the metabolism of terfenadine may not be limited to a single enzyme and/or the enzyme(s) are not fully inhibited by ketoconazole. Based on the almost complete inhibition of formation of M1, M5, M6, and M8 in locusts (Fig. 4), it seems likely that alternative metabolic pathways take part in terfenadine metabolism.

M3 and M10 were tentatively identified as glucose conjugates of terfenadine alcohol (M5) and terfenadine, respectively. In hemolymph the concentration was too low to be followed over time suggesting that the excretion rate for this metabolite is high or that M3 is further metabolized. M10 increased significantly after 20 minutes from injection time compared with the amount in locusts receiving only terfenadine. The excreted amount of M3 was not significantly inhibited by ketoconazole even though the formation of M5 was significantly inhibited. M10 was increased in the presence of the CYP3A4 inhibitor. This is in agreement with the findings that other metabolic pathways are inhibited and thus that more terfenadine was available for glycosylation. However, the excreted amount of glucoside metabolites may be misleading due to glycosidase activity in the intestine (Kikal and Smith, 1959).

Previously, conjugates with amino acids, glucose, phosphate, and sulfate have been reported in insects (Myers and Smith, 1954; Smith, 1955, 1962; Cohen and Smith, 1964; Ngah and Smith, 1983). Glycosylation is mentioned a number of times in the literature as a detoxification mechanism in insects. Glycosylation can conjugate to amines and hydroxyl and carboxy groups (Smith, 1968) and has been suggested to be analogous to mammalian glucuronidation (Smith, 1962). Although glucuronic acid conjugates have been reported in insects (Terriere et al., 1961), it has later been questioned in the literature (Lowenstein, 1968). Due to inadequate identification tools available in the 1950s and 1960s, metabolites may have been wrongly identified as glucuronic acid conjugates.

It has been tested whether terfenadine and other tertiary amines could be metabolized into *N*-glucuronides (Luo et al., 1991). The study was conducted on healthy volunteers, and for eight of the nine compounds tested glucuronides were detected in the urine. Terfenadine was the only compound of the nine tertiary amines tested that was not metabolized by the glucuronidation pathway. Glucoside formation has been reported in humans, although the detoxification mechanism generally is considered to be characteristic in invertebrates and other lower organisms (Gessner et al., 1973). Based on the results in our study regarding substrate specificity, glucuronidation in mammals does not appear to be analogous to glycosylation in insects as no glucuronides of terfenadine have been reported. However, the two detoxification mechanisms are probably evolutionarily related (Smith, 1968).

Phosphate and sulfate metabolites have been reported in insects (Smith, 1955; Ngah and Smith, 1983). Phosphate and sulfate conjugates of the same compound differ in mass by only 10 mmu. With accurate mass techniques we were able to distinguish between these two adducts. Thus, M9, M11, and M12 were tentatively identified as phosphate conjugates of M5 (terfenadine alcohol), M7, and terfenadine, respectively. Assuming the MS responses of terfenadine and the metabolites are somewhat similar, M9 was the most abundant metabolite found in locust feces and hemolymph (Figs. 5 and 6). In Figs. 5 and 6 it appears that the formation of M9 and M11 is significantly inhibited by ketoconazole, possibly due to inhibition of the oxidation step.

The structure of M7 was not confirmed by NMR, and it is possible that the carbonyl consists of a ketone rather than an aldehyde, which is shown in Fig. 9.

The formation of M12 in hemolymph was initially inhibited by ketoconazole even though P450 is not expected to be involved and no hydroxylation is required (Fig. 5). However, the amount excreted in feces was not significantly different when the locusts were given ketoconazole (Fig. 6). Looking at Fig. 5, it appears that there is a large increase in the amount M12 between 60 and 120 minutes postinjection when ketoconazole is coadministered.

No sulfate metabolites of terfenadine were identified. Based on the present results, conjugation with phosphate and glucose seems to be a major phase II detoxification pathway in locusts. These metabolites are qualitatively different from mammalian metabolic pathways and appear to some extent to take over from P450 enzymes when these enzymes are inhibited.

Although many insecticides, such as dimethoate, have been developed due to the formation of toxic metabolites in insects but not in mammals (Smith, 1968), the phase I metabolism of terfenadine in locusts resembles mammalian phase I metabolism. It is therefore possible that the insect model could be used in phase I metabolism investigations and not only be useful for determining BBB permeation. Locusts may also be used in generating human-relevant metabolites for further identification. However, extensive characterization of the insect models is necessary to determine their applicability. Inclusion of insect experiments in early preclinical drug development could possibly reduce costs as fewer "poor" candidates would proceed to in vivo experiments in mammals. In the present study, we have shown that locusts may have an enzyme with functionality similar to mammalian CYP3A4, an important enzyme involved in the human metabolism of almost half of marketed drugs (Guengerich, 2008).

Authorship Contributions

Participated in research design: Olsen, Hansen, Badolo, Gabel-Jensen.
Conducted experiments: Olsen.
Contributed new reagents or analytic tools: Hansen.
Performed data analysis: Olsen, Hansen, Badolo.
Wrote or contributed to the writing of the manuscript: Olsen, Hansen, Badolo, Gabel-Jensen, Nielsen.

References

Alavijeh MS, Chishty M, Qaiser MZ, and Palmer AM (2005) Drug metabolism and pharmacokinetics, the blood-brain barrier, and central nervous system drug discovery. *NeuroRx* **2**: 554–571.

Andersson O, Hansen SH, Hellman K, Olsen LR, Andersson G, Badolo L, Svenstrup N, and Nielsen PA (2013) The grasshopper: a novel model for assessing vertebrate brain uptake. *J Pharmacol Exp Ther* **346**:211–218.

Cohen AJ and Smith JN (1964) Comparative detoxication. 9. The metabolism of some halogenated compounds by conjugation with glutathione in the locust. *Biochem J* **90**:449–456.

Feyereisen R (1999) Insect P450 enzymes. *Annu Rev Entomol* **44**:507–533.

Geldenhuys WJ, Allen DD, and Bloomquist JR (2012) Novel models for assessing blood-brain barrier drug permeation. *Expert Opin Drug Metab Toxicol* **8**:647–653.

Gessner T, Jacknowitz A, and Vollmer CA (1973) Studies of mammalian glucoside conjugation. *Biochem J* **132**:249–258.

Guengerich FP (2008) Cytochrome p450 and chemical toxicology. *Chem Res Toxicol* **21**:70–83.

Honig PK, Wortham DC, Zamani K, Conner DP, Mullin JC, and Cantilena LR (1993) Terfenadine-ketoconazole interaction. Pharmacokinetic and electrocardiographic consequences. *JAMA* **269**:1513–1518.

Hughes JP, Rees S, Kalindjian SB, and Philpott KL (2011) Principles of early drug discovery. *Br J Pharmacol* **162**:1239–1249.

Jurima-Romet M, Crawford K, Cyr T, and Inaba T (1994) Terfenadine metabolism in human liver. In vitro inhibition by macrolide antibiotics and azole antifungals. *Drug Metab Dispos* **22**: 849–857.

Jurima-Romet M, Wright M, and Neigh S (1998) Terfenadine-antidepressant interactions: an in vitro inhibition study using human liver microsomes. *Br J Clin Pharmacol* **45**:318–321.

Kikal T and Smith JN (1959) Comparative detoxication. 6. The metabolism of 6-amino-4-nitro-o-cresol and 4:6-dinitro-o-cresol in locusts. *Biochem J* **71**:48–54.

Klowden MJ (2007) *Physiological Systems in Insects*, Elsevier, Amsterdam.

Lee RM (1961) The variation of blood volume with age in the desert locust (Schistocerca gregaria Forsk.). *J Insect Physiol* **6**:36–51.

Ling KH, Leeson GA, Burmaster SD, Hook RH, Reith MK, and Cheng LK (1995) Metabolism of terfenadine associated with CYP3A(4) activity in human hepatic microsomes. *Drug Metab Dispos* **23**:631–636.

Lowenstein O, editor (1968) *Advances in Comparative Physiology and Biochemistry*, vol 3, Academic Press, New York.

Luo H, Hawes EM, McKay G, Korchinski ED, and Midha KK (1991) N(+)-glucuronidation of aliphatic tertiary amines, a general phenomenon in the metabolism of H1-antihistamines in humans. *Xenobiotica* **21**:1281–1288.
Myers CM and Smith JN (1954) Comparative detoxication. II. Glucoside formation from phenols in locusts. *Biochem J* **56**:498–503.
Naik P and Cucullo L (2012) In vitro blood-brain barrier models: current and perspective technologies. *J Pharm Sci* **101**:1337–1354.
Ngah WZ and Smith JN (1983) Acidic conjugate of phenols in insects; glucoside phosphate and glucoside sulphate derivatives. *Xenobiotica* **13**:383–389.
Nielsen PA, Andersson O, Hansen SH, Simonsen KB, and Andersson G (2011) Models for predicting blood-brain barrier permeation. *Drug Discov Today* **16**:472–475.
Raeissi SD, Guo Z, Dobson GL, Artursson P, and Hidalgo IJ (1997) Comparison of CYP3A activities in a subclone of Caco-2 cells (TC7) and human intestine. *Pharm Res* **14**:1019–1025.
Rodrigues AD, Mulford DJ, Lee RD, Surber BW, Kukulka MJ, Ferrero JL, Thomas SB, Shet MS, and Estabrook RW (1995) In vitro metabolism of terfenadine by a purified recombinant fusion protein containing cytochrome P4503A4 and NADPH-P450 reductase. Comparison to human liver microsomes and precision-cut liver tissue slices. *Drug Metab Dispos* **23**: 765–775.
Scott JG (2008) Insect cytochrome P450s: thinking beyond detoxification, in *Recent Advances in Insect Physiology, Toxicology and Molecular Biology* (Liu N ed) pp 117–124, Research Signpost, Kerala, India.
Scott JG and Wen ZM (2001) Cytochromes P450 of insects: the tip of the iceberg. *Pest Manag Sci* **57**:958–967.
Shibata Y, Takahashi H, Chiba M, and Ishii Y (2008) A novel approach to the prediction of drug-drug interactions in humans based on the serum incubation method. *Drug Metab Pharmacokinet* **23**:328–339.
Smith JN (1955) Comparative detoxication. 4. Ethereal sulphate and glucoside conjugations in insects. *Biochem J* **60**:436–442.
Smith JN (1962) Detoxication mechanisms. *Annu Rev Entomol* **7**:465–480.
Smith JN (1968) The comparative metabolism of xenobiotics. *Adv Comp Physiol Biochem* **3**: 173–232.
Terriere LC, Boose RB, and Roubal WT (1961) The metabolism of naphthalene and 1-naphthol by houseflies and rats. *Biochem J* **79**:620–623.
Wilkinson CF and Brattsten LB (1972) Microsomal drug-metabolizing enzymes in insects. *Drug Metab Rev* **1**:153–227.

Address correspondence to: Line Rørbæk Olsen, Department of Pharmacy, Faculty of Health and Medical Sciences, University of Copenhagen, DK-2100 Copenhagen, Denmark. E-mail: line.olsen@sund.ku.dk